Periodic Motion Control for Monorotor type Flying Robot at Non-equilibrium Point via Zero Dynamics Controller

Yasuyuki Kataoka[1], Kazuma Sekiguchi[1] and Mitsuji Sampei[1]

[1]Department of Mechanical and Control System Engineering, Tokyo Institute of Technology, Tokyo, Japan
(Tel: +81-90-4223-9731; E-mail: kataoka@sc.ctrl.titech.ac.jp)
(Tel: +81-80-3392-6379; E-mail: sekiguchi@ctrl.titech.ac.jp)
(Tel: +81-3-5734-2552; E-mail: sampei@ctrl.titech.ac.jp)

Abstract: This paper proposes a nonlinear controller realizing periodic motion to MonoRotor type flying robot having no equilibrium point. The control target is semi-hovering; a motion that passes a desired non-equilibrium point at which position and attitude stop periodically. In order to achieve this control objective, we propose discontinuous and time-varying output zeroing controller which ends up controlling Zero Dynamics. The numerical simulation and stability analysis show the validity of the suggesting controller design method.

Keywords: Nonlinear Control, Underactuated System, Zero Dynamics, Flying robot, Periodic Motion

1. INTRODUCTION

This paper discusses a new nonlinear controller design method of periodic motion control for Monorotor type flying robot; a simple model of flying robot composed of both a body mass and a rotor. This system has structural underactuation, since the number of input is less than the number of states. In addition, Monorotor robot does not own the equilibrium point. Because of these properties, the only way to realize the meaningful motion is semi-hovering shown in Fig.1, which is a periodic motion that passes at the desired non-equilibrium point in each cycle. This control objective requires Zero Dynamics to be controlled. The main contribution of this paper is the controller design that results in controlling Zero Dynamics.

One of the researches regarding the periodic motion has been done by A. Shiriaev [1]. They derived the sufficient conditions that Zero Dynamics becomes periodic dynamics when time-invariant output zeroing control is applied. Their theorem requires the existence of the equilibrium point in the system, whereas this paper gives an example to control Zero Dynamics by time-variant output function against the system that does not have equilibrium point.

The composition of this paper is as follows. First, modeling and system analysis in section 2 and 3 reveal that this system does not have equilibrium point, meaning it does not own locally asymptotically stabilizability(LAS). This result let the controller design for Monorotor robot focus on realization of periodic motion. Second, the design method of Zero Dynamics Control, the main contribution of this paper, is shown in section 4. The idea of controller design is changing output function discretely with maintaining continuity of output function and derivative of it at each boundary. This design method indicates one of the solutions to control Zero Dynamics.

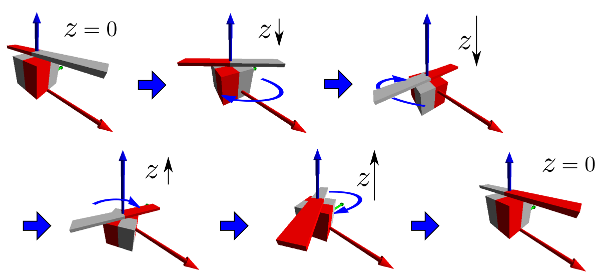

Fig. 1 Semi Hovering Motion

Table 1 Physical Variables

z	: position of center of body mass [m]
ψ	: posture angle of body mass [rad]
θ_p	: relative angle of rotor [rad]
τ	: input torque to rotor [N·m]

Table 2 Physical Parameters

m	: mass of body	: 0.10 [kg]
J_r	: inertial moment of body	: 0.150 [kg·m^2]
J_p	: inertial moment of rotor	: 0.050 [kg·m^2]
k_p	: coefficient of property of rotor	: 0.10 [kg/m]
g	: gravity force	: 9.8 [kgm^2]

2. MODELING

In this section, nonlinear state equation of Monorotor robot is given under some assumptions. First, the physical variables and parameters are defined in Table1 and Table2. The physical image of the states is shown in Fig.2. Next, three assumptions to the Monorotor robot is given as follows.

1. Propulsion Force generated by Rotors
   Translational force generated by the main rotor is proportional to square of the angular velocity of the rotor. This assumption is based on aerodynamics shown in [4]. The propulsion force is given by

$$F_m = k_p(\dot{\psi} + \dot{\theta}_p)^2 \mathrm{sgn}\left(\dot{\psi} + \dot{\theta}_p\right) \quad (1)$$

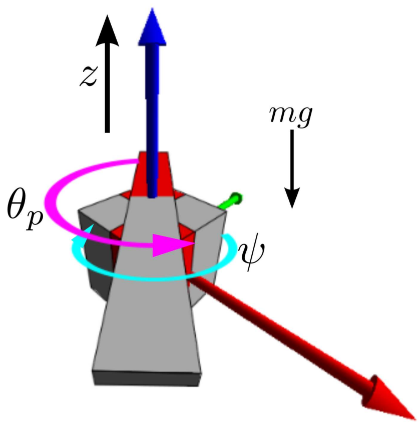

Fig. 2 MonoRotor Model

, where k_p is a constant parameter that determines the physical property of the rotor. Note that the positive rotation generates positive translational force and vice versa.

2. Counteraction against Input Torque
   The counteraction against input torque can not be neglected for this system, since the inertia of this vehicle is assumed to be relatively small to the input torque.
3. Neglect of air resistance
   It is assumed that Monorotor robot does not have the damping term in the system dynamics. This assumption comes from the simplification of the system dynamics.

In order to derive the nonlinear state equation, first of all, let $\boldsymbol{x}_m$ denote the state of the Monorotor robot,

$$\boldsymbol{x}_m =: [z, \psi, \dot{z}, \dot{\psi}, \dot{\theta}_p]^T \in \mathbb{R}^4 \times \mathbb{S}^1 \tag{2}$$

. Note that θ_p can be neglected from system realization because it, apparently, does not affect system dynamics. The dynamics of Monorotor robot can be derived via Lagrange-Euler method and it results in

$$\frac{\mathrm{d}}{\mathrm{dt}}\begin{bmatrix} z \\ \psi \\ \dot{z} \\ \dot{\psi} \\ \dot{\theta}_p \end{bmatrix} = \begin{bmatrix} \dot{z} \\ \dot{\psi} \\ \frac{k_p(\dot{\psi}+\dot{\theta}_p)^2 \mathrm{sgn}(\dot{\psi}+\dot{\theta}_p)}{m} - g \\ 0 \\ 0 \end{bmatrix} + \begin{bmatrix} 0 \\ 0 \\ 0 \\ -\frac{2}{J_r} \\ \frac{J_r+2J_p}{J_pJ_r} \end{bmatrix}\tau$$
$$= \boldsymbol{f}_m(\boldsymbol{x}_m) + \boldsymbol{g}_m\tau \tag{3}$$

Hereby, it is easily shown that Monorotor robot owns non-holonomic constraint (4) by computing (3),

$$\dot{\theta}_p(t) = -\frac{J_r + 2J_p}{2J_p}\left(\dot{\psi}(t) - \dot{\psi}(t_k)\right) + \dot{\theta}_p(t_k) \tag{4}$$

, where t_k represents the initial time. This constraint let the original dynamical model (3) transform to 4 dimensional which is

$$\frac{\mathrm{d}}{\mathrm{dt}}\begin{bmatrix} z \\ \psi \\ \dot{z} \\ \dot{\psi} \end{bmatrix} = \begin{bmatrix} \dot{z} \\ \dot{\psi} \\ \frac{k_p\alpha(t)^2}{m}\mathrm{sgn}(\alpha(t)) - g \\ 0 \end{bmatrix} + \begin{bmatrix} 0 \\ 0 \\ 0 \\ -\frac{2}{J_r} \end{bmatrix} u \tag{5}$$

$$\alpha(t) = -\frac{J_r}{2J_p}\dot{\psi}(t) + \frac{J_r + 2J_p}{2J_p}\dot{\psi}(t_k) + \dot{\theta}_p(t_k) \tag{6}$$

$$\frac{\mathrm{d}}{\mathrm{dt}}\boldsymbol{x} = \boldsymbol{f}(\boldsymbol{x}) + \boldsymbol{g}\tau,\ \boldsymbol{f}(\boldsymbol{x}) \in \mathbb{R}^{4\times1},\ \boldsymbol{g} \in \mathbb{R}^{4\times1} \tag{7}$$

, where $\boldsymbol{x} = [z, \psi, \dot{z}, \dot{\psi}]^T \in \mathbb{R}^3 \times \mathbb{S}$ denotes the new reduced state.

3. SYSTEM ANALYSIS

This section briefly reveals the property of Monorotor robot and indicates the control objective for Monorotor robot.

3.1 Equilibrium point and LAS

First, it is easily shown from (7) that there does not exist equilibrium point in Monorotor robot, since there are no $\boldsymbol{x}$ and τ that satisfies $\boldsymbol{f}(\boldsymbol{x}) + \boldsymbol{g}\tau = 0$. This result also verifies that Monorotor model does not own Locally Asymptotically Stabilizability(LAS), because the existence of the equilibrium point is the necessary condition for LAS. Hence, it is implied that the control target needs to be shifted to the stable periodic motion passing non-equilibrium point in each cycle.

4. CONTROLLER DESIGN

This section gives the new nonlinear controller design that controls Zero Dynamics.

4.1 Basic Control Strategy

Let "semi-hovering", the control objective, be defined as "a motion that passes a desired non-equilibrium point at which position and attitude stop periodically". The target non-equilibrium point for the semi-hovering can be selected as

$$\boldsymbol{q}_m^* = \left[0, 0 + 2\pi k, 0\right] (k : \text{integer}) \tag{8}$$

without loss of generalization due to $\psi \in \mathbb{S}$.

As the basic strategy to realize semi-hovering, the following two steps are considered.

1^{st} step : Control posture angle ψ
2^{nd} step : Synchronize position x with posture angle ψ
Remark that this control strategy requires the realization of 1^{st} step to be kept, when 2^{nd} step is being focused.

4.2 1^{st} step: Control posture via Output Zeroing

First, in order to discuss a cycle in periodic motion explicitly, let $k := [t_k, t_{k+1}]$ be defined as a closed section k . Plus, let $\psi_r^{\{k\}}(t)$ be a desired trajectory of posture angle ψ in a section k.

Next, the output function that realizes 1^{st} step is designed. Since ψ is cylinder coordinates, ψ does not have to converge as long as $\dot{\psi} = 0$ is satisfied in each cycle.

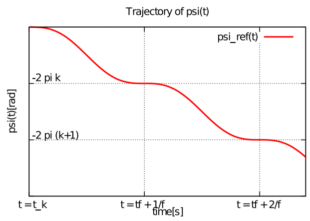

Fig. 3 trajectory $\psi_r(t)$

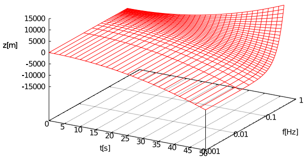

Fig. 4 t-f-z simulation graph

Thus, one of the candidates of the output function satisfying the above condition is given by

$$h^{\{k\}}(\boldsymbol{x},t) = \psi(t) - \psi_r^{\{k\}}(t) \tag{9}$$

$$\psi_r^{\{k\}}(t) = \sin(2\pi f(t-t_k)) - 2\pi f(t-t_k) \tag{10}$$

, where $h^{\{k\}}(\boldsymbol{x},t)$ represents the output function in a section k and f denotes the frequency of the rotation of the body mass.

Fig.8 is the image of the reference trajectory of (10). Since the relative degree of the output function (9) is 2, the output zeroing input in a section k is computed by (11). The details can be found in [2] or [3].

$$u^{\{k\}}(\boldsymbol{x},t) = \frac{-(L_f^2 h^{\{k\}}(\boldsymbol{x},t) - \ddot{\psi}_r^{\{k\}}(t)) + v}{L_g L_f h^{\{k\}}(\boldsymbol{x},t)} \tag{11}$$

As a result of input output linearization gained by superimposing (11), the system turns into (12) having linear subsystem and nonlinear subsystem, that is,

$$\frac{\mathrm{d}}{\mathrm{dt}}\begin{bmatrix} h^{\{k\}}(\boldsymbol{x},t) \\ \dot{h}^{\{k\}}(\boldsymbol{x},t) \\ z \\ \dot{z} \end{bmatrix} = \begin{bmatrix} \dot{\xi} \\ \ddot{\xi} \\ \dot{\eta} \\ \ddot{\eta} \end{bmatrix} = \begin{bmatrix} \begin{bmatrix} 0 & 1 \\ 0 & 0 \end{bmatrix}\begin{bmatrix} \xi \\ \dot{\xi} \end{bmatrix} + \begin{bmatrix} 0 \\ 1 \end{bmatrix} v \\ \begin{bmatrix} \boldsymbol{q}_{z1}(\boldsymbol{\xi},\boldsymbol{\eta},t) \\ \boldsymbol{q}_{z2}(\boldsymbol{\xi},\boldsymbol{\eta},t) \end{bmatrix} \end{bmatrix} \tag{12}$$

, where $\boldsymbol{\xi} = [\xi, \dot{\xi}]^T$ is *External Dynamics* and $\boldsymbol{\eta} = [\eta, \dot{\eta}]^T$ is *Internal Dynamics* which is expressed as $\boldsymbol{q}_{z1}(\boldsymbol{\xi},\boldsymbol{\eta},t)$ and $\boldsymbol{q}_{z2}(\boldsymbol{\xi},\boldsymbol{\eta},t)$ respectively. Remark that $\boldsymbol{\eta}$ is called *Zero Dynamics* when the outputzeroing control is achieved($\xi = 0, \dot{\xi} = 0$).

Maintaining the output zeroing constrains the dynamics of the posture, that is,

$$\psi^{\{k\}} = \sin(2\pi f t) - 2\pi f t \tag{13}$$

$$\dot{\psi}^{\{k\}} = 2\pi f \cos(2\pi f t) - 2\pi f \tag{14}$$

. The most important feature of this control is that the behavior of the position, Zero Dynamics, depends on the frequency in (10). The Fig.4 shows the numerical simulation of the time response of the position z with the parameter variation of f. As is shown, the behavior of Zero Dynamics, position z, can be controlled by changing f.

4.3 2nd step : Zero Dynamics Control

Let $f^{\{k\}}$ denote the frequency in the section k : $[t_k, t_{k+1}]$. Thus, the desired trajectory in the section k needs modification. The new desired trajectory $\psi_r^{\{k\}}(t)$ becomes

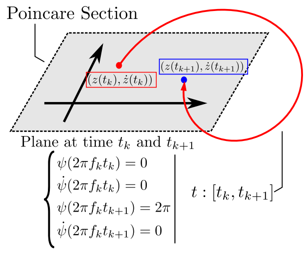

Fig. 5 poincaré plane

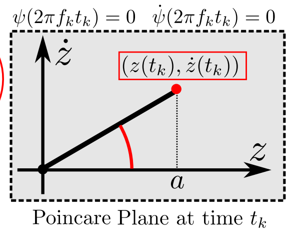

Fig. 6 image of $f^{\{k\}}$

$$\psi_r^{\{k\}}(t) = \sin(2\pi f^{\{k\}}(t-t_k)) - 2\pi f^{\{k\}}(t-t_k) \tag{15}$$

. Here, remark that the continuity of output function and the derivatives of them until second time derivative is guaranteed on the boundary of each section k. This feature enables linear subspace to be kept zero even though the parameter variation against $f^{\{k\}}$ is implemented at the boundary of the section, meaning Zero Dynamics can be simply controlled by designing parameter $f^{\{k\}}$ discretely. Thus, let $f^{\{k\}}$ be called as virtual discontinuous input to Zero Dynamics in this paper.

The Zero Dynamics of this system is analytically computed by integration of $\ddot{\eta}$.

$$\text{if } \dot{\psi}(t-t_k) > 2\frac{J_p}{J_r}\dot{\theta}_p(t_k) + \frac{J_r + 2J_p}{J_r}\dot{\psi}(t_k)$$

$$z(t-t_k) = a_2(t-t_k)^2 - a_1(t-t_k) + a_0 \tag{16}$$

$$\text{else } z(t-t_k) = b_2(t-t_k)^2 - b_1(t-t_k) + b_0 \tag{17}$$

where $a_i, b_i (i = 0,1,2)$ are constant parameters depending on the designed parameter $f^{\{k\}}$ and the initial conditions $z(t_k)$,$\dot{z}(t_k)$, $\psi(t_k)$ and $\dot{\psi}(t_k)$.

Using the result of Zero Dynamics analysis, (16) and (17), the discrete Zero Dynamics at section k is driven as follows.

$$\begin{bmatrix} z[k+1] \\ \dot{z}[k+1] \end{bmatrix} = \boldsymbol{A}_d \begin{bmatrix} z[k] \\ \dot{z}[k] \end{bmatrix} + \boldsymbol{B}_d \tag{18}$$

$$\boldsymbol{A}_d = \begin{bmatrix} 1 & \frac{1}{f^{\{k\}}} \\ 0 & 1 \end{bmatrix}, \boldsymbol{B}_d = \begin{bmatrix} B_{11}\frac{1}{f^{\{k\}}}^2 + B_{12}\frac{1}{f^{\{k\}}} + B_{13} \\ B_{21}\frac{1}{f^{\{k\}}} + B_{22} + B_{23}f^{\{k\}} \end{bmatrix} \tag{19}$$

Unfortunately, since there is no way to design controller to stabilize (18) by well-known systematic design method, it becomes necessary to use different approach.

The way to design $f^{\{k\}}$ is based on the poincaré space satisfying $\psi = 0, \dot{\psi} = 0$ shown in Fig.5 and Fig.6.

$$f^{\{k\}} = f_z^{\{k\}} a + f_{dz}^{\{k\}}(1-a) \tag{20}$$

$$a = \cos\left(\tan^{-1}\left(\frac{|\dot{z}(t_k)|}{|z(t_k)|}\right)\right)$$

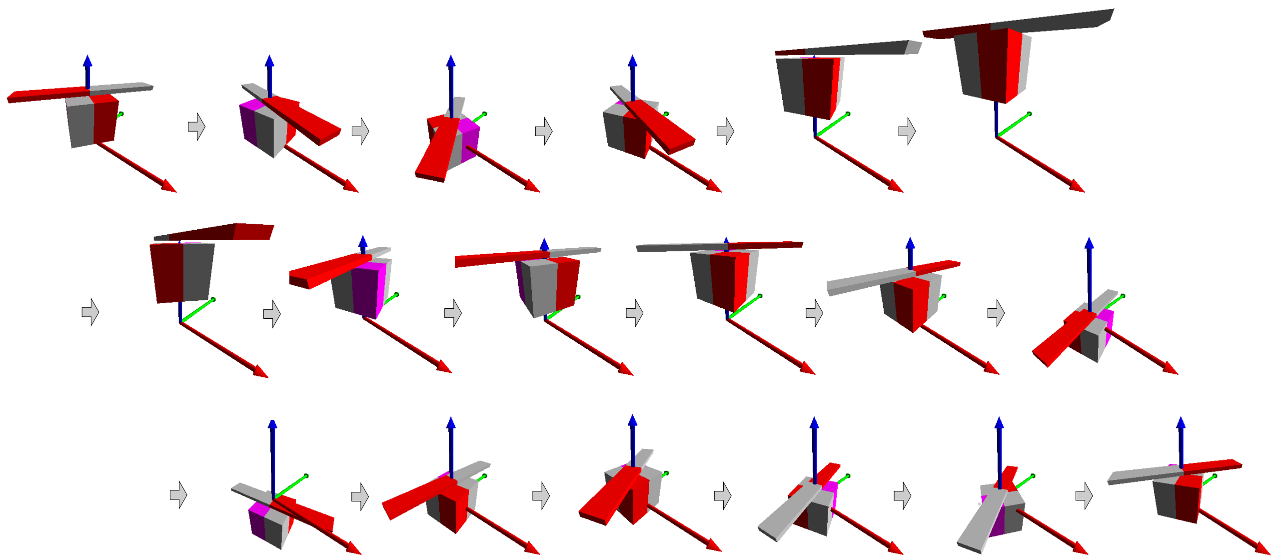

Fig. 7 Position and Attitude Control via Discrete Output Zeroing Control; Semi-Hovering Control

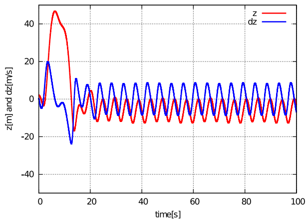

Fig. 8 $z(t)$ and $\dot{z}(t)$

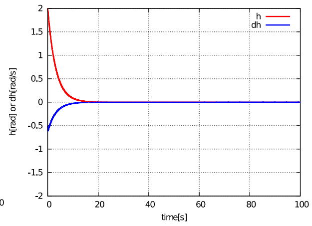

Fig. 9 $h(\boldsymbol{x}, t)$ and $\dot{h}(\boldsymbol{x}, t)$

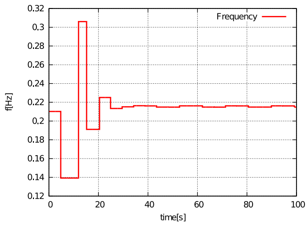

Fig. 10 Frequency f

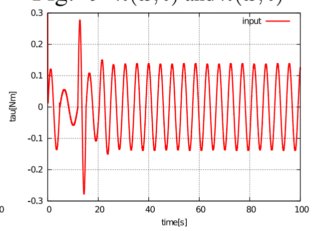

Fig. 11 torque input[N·m]

where $f_z^{\{k\}}$ is the frequency satisfying $z(t_{k+1}) = 0$ and $f_{dz}^{\{k\}}$ is the frequency satisfying $\dot{z}(t_{k+1}) = 0$ at $t_{k+1} = t_k + \frac{1}{f_k}$. Both can be analytically derived from (16) and (17), respectively. It is expected that the frequency $f^{\{k\}}$ gradually converges through updating the virtual discontinuous input, $f^{\{k\}}$, in each interval.

5. NUMERICAL SIMULATION

The physical parameters used in this numerical simulation are given in Table2. The initial condition is

$$\boldsymbol{x}_m(0) = [2.0, 2.0, 0.5, -0.5, 2.0]^T \tag{21}$$

. According to Fig.8, it is confirmed that both z and ψ are synchronized with each other. This result shows the Zero Dynamics is controlled via virtual discontinuous input $f^{\{k\}}$. addition, Fig.9 and Fig.10 show that the realization of 1^{st} step to be kept in the 2^{nd} step.

5.1 Numerical Stability analysis

The poincaré map is shown in Fig.12 and Fig.13. Zero Dynamics, z and $\dot{z}$, is almost zero though, it does not

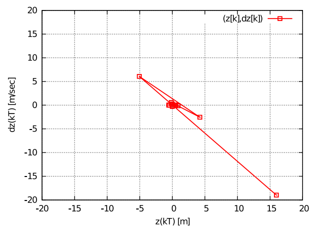

Fig. 12 poincaré map

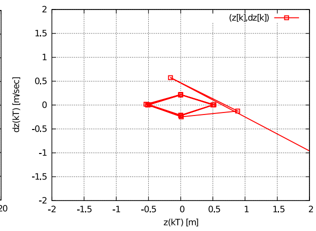

Fig. 13 precise poincaré map

technically converge. However, periodic motion can be said to be achieved by considering four cycle as one cycle. Thus, it is concluded that stable periodic motion is obtained by the suggesting nonlinear controller.

6. CONCLUSION

In this paper, a new way to design time-varying nonlinear controller that realize periodic motion is proposed. This method also suggests a way to control Zero Dynamics for Monorotor type flying robot. Numerical simulation verified the validity of the suggesting controller, achieving semi-hovering motion successfully.

REFERENCES

[1] A. Shiriaev and A. Robertsson and J. Perram and A. Sandberg, "Periodic motion planning for virtually constrained Euler-Lagrange systems", *Systems & Control Letters*, Vol.55, No.11, pp.900–907, Nov. 2006.

[2] Hassan K.Khalil, "Nonlinear Systems, Third Edition", *Prentice Hall*, chap.13

[3] Alberto Isidori, "Nonlinear Control Systems", *Springers*, chap. 2

[4] John J.Bertin, "Aerodynamics for Engineers(4th Edition)", *Prentice Hall*

[5] Herbert Goldstein, "Classical Mechanics, Second Edition", *Addison-Wesley Publishing Company*, chap. 4&5